

Direct Evidence of Water-Assisted Sintering of Cobalt on Carbon Nanofiber Catalysts during Simulated Fischer–Tropsch Conditions Revealed with in Situ Mössbauer Spectroscopy

G. Leendert Bezemer,* Tom J. Remans, Alexander P. van Bavel, and A. Iulian Dugulan

Shell Technology Centre Amsterdam, Grasweg 31, 1031 HW Amsterdam, The Netherlands and Reactor Institute Delft, Delft University of Technology, Mekelweg 15, 2629 JB Delft, The Netherlands

Received April 9, 2010; E-mail: Leendert.Bezemer@Shell.com

In the Fischer–Tropsch (FT) reactions CO and H₂ are catalytically converted into hydrocarbons and water via surface polymerization. Using this process high-grade transportation fuels can be produced from biomass, coal, or natural gas. For this reason the FT process receives much attention in both academia and industry.¹ Gas-To-Liquids (GTL), for which supported cobalt catalysts are preferred, is of growing importance for the global energy supply with a combined capacity of both current plants and plants under construction of ~250,000 bpd.

The most important contributors to deactivation of cobalt FT catalysts are thought to be coke formation, oxidation, poisoning, and sintering.² The role of water, the main product in the FT reaction, on deactivation is still not clear. Thermodynamic calculations have shown that nanosized cobalt particles can be oxidized by water at the prevailing H₂O/H₂ ratio at FT conditions, although others refuted that oxidation of cobalt is a deactivation mechanism during industrial operation.³ However, the question remains whether small metallic cobalt particles have a higher tendency to oxidize compared to larger particles. To elucidate the role of water in the deactivation of cobalt Fischer–Tropsch catalysts we investigated the cobalt chemical state of well-defined catalysts at 20 bar and 200–220 °C using different H₂O/H₂ ratios applying Mössbauer emission spectroscopy. As support, material graphitic carbon nanofibers (CNFs) are used. On CNFs it is possible to obtain a highly dispersed cobalt phase that is fully reducible.⁴

Co/CNF catalysts with a metal loading of 8 wt % were synthesized in duplicate applying aqueous Co(NO₃)₂ impregnation both with and without 90 MBq radioactive ⁵⁷Co added. The resulting four catalysts were pairwise used in the study to enable the collection of Mössbauer spectra from the radioactive sample and conventional catalyst characterization data from the nonradioactive sample. The cobalt dispersion as measured with hydrogen chemisorption was 19% (5.1 nm). In Figure 1a, a representative HAADF TEM image of the reduced and passivated catalyst is depicted. The bright areas in the left image reflect high density material and stem from the cobalt crystallites as was proven by EDX measurement. A histogram with cobalt particle size distributions of the fresh and the spent catalyst is presented in Figure 1b. The resulting surface average particle size was 5.0 nm, supporting the chemisorption data. From the TEM image it becomes clear that the fibers have an inner tube with a diameter of ~6–7 nm. Following earlier results with Co/CNF we estimate that 15% of the cobalt is located in the inner tube.⁵ The cobalt particles in the inner tube are accessible for reactants, as will become clear from the Mössbauer data (vide supra).

The Mössbauer spectrum of the catalyst after reduction at 350 °C is given in Figure 2. The signal is composed of a singlet (42%) stemming from very small super paramagnetic (SPM) cobalt particles and a sextuplet (58%) coming from larger cobalt particles

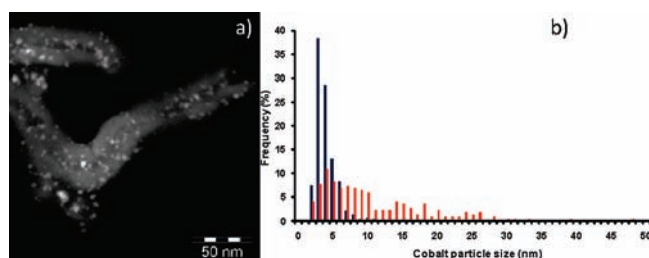


Figure 1. (a) TEM image obtained with the HAADF detector of the freshly reduced catalyst. The cobalt particles appear as white spots. (b) Histogram of particle size distribution in fresh and spent catalyst.

which are magnetically ordered. From comparison of these results with the particle size distribution for TEM it can be concluded that the switch from superparamagnetic to magnetic ordered cobalt takes place at ~5 nm, which is comparable to a value at 6 nm for α -Fe on carbon.⁶ The presence of two contributors in the Mössbauer signal is very helpful to draw conclusions on the impact of cobalt particle size on catalyst deactivation.

After reduction the reactor was pressurized to 20 bar and at 220 °C the catalyst was exposed to a gas stream of H₂O, H₂, and Ar. First we verified the Mössbauer spectrum, which showed unchanged contributions of a singlet and sextuplet, indicating that the cobalt species have similar Debye temperatures. Subsequently the H₂O/H₂ ratio was systematically increased from 1, 2, 4, 10, to 30 and at each condition the Mössbauer signal was measured during 4 days. In Figure 2 the signal during the treatment with highest oxidizing power is presented. The shape of both cobalt species did not change, clearly showing that oxidation was completely absent up to this very high H₂O/H₂ ratio. In industrial Fischer–Tropsch conditions the H₂O/H₂ ratio is ~1, which clearly confirms that oxidation is not a deactivation mechanism during commercial operation, even for the smallest cobalt crystallites. However, when the hydrogen flow was closed oxidation did take place. The shape and position of both the SPM and the larger cobalt clusters changed completely; see Figure 2c. During the first day of the H₂O-only treatment all SPM cobalt particles were oxidized, as well as part of the larger particles, whereas a day later the oxidation to CoO was complete. This clearly shows that oxidation of cobalt by water is possible, but only in the absence of hydrogen.

The experiment was continued by reduction of the catalyst by hydrogen at 350 °C after which the Mössbauer spectrum showed fully reduced cobalt. Now again a gas flow with a H₂O/H₂ ratio of 1 was passed over the catalyst. This new condition was at a significantly higher relative humidity (RH). The RH is defined as the ratio of the partial pressure of water vapor to the saturated vapor pressure of water at a certain temperature and pressure. In our experiments the RH was varied by changing the inert concentration.

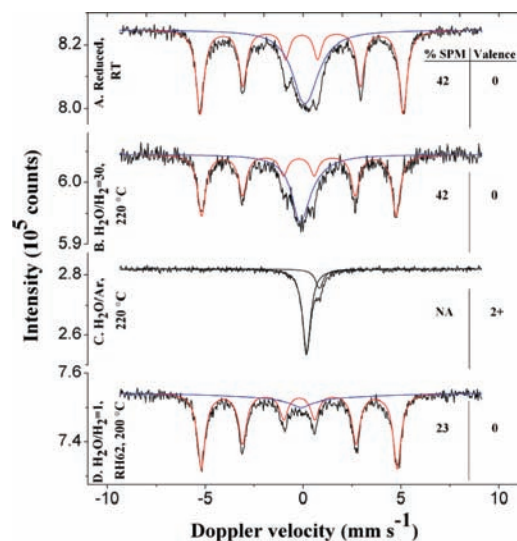


Figure 2. Mössbauer emission spectra measured after reduction and at conditions with varying $\text{H}_2\text{O}/\text{H}_2$ ratio. Spectra are fitted with a super paramagnetic (blue) and a magnetic ordered (red) contributor.

All earlier conditions were conducted at a low RH of 25%, but now the gas flows were adjusted to reach an RH of 62%. The impact of this change of the RH on the system is great. Within 1 week the SPM spectral contribution decreased to 23% as can be seen in Figure 2d. The decrease of the SPM contribution and the increase of the magnetically ordered signal from the larger particles can be ascribed to sintering. Not only did the fraction of bulk cobalt increase, but also its average particle size, evident from the increase in hyperfine field (see Supporting Information). It is important to note that no oxidation effect was observed and that sintering involved metallic phases.

The activity for the FT reaction of the deactivated catalyst was measured at 220 °C at 1 bar using a H_2/CO ratio of 2 and compared with the activity of a freshly reduced sample. The activity of the catalyst had more than halved, from 2.3×10^{-5} to 1.1×10^{-5} $\text{mol}_{\text{CO}}/\text{g}_{\text{Co}} \cdot \text{s}$. In fact, the actual deactivation is even stronger, as initially the sintering of the smallest particles will increase activity. This is due to the much lower TOF associated with particles smaller than 6 nm in the FT reaction, outweighing a small change in the dispersion.⁴ A TOF of $12 \times 10^{-3} \text{ s}^{-1}$ is obtained for catalysts with particles larger than 6 nm.⁴ From our measured TOF of $7.1 \times 10^{-3} \text{ s}^{-1}$ we estimated that the activity of the fresh catalyst would have been $4.0 \times 10^{-5} \text{ mol}_{\text{CO}}/\text{g}_{\text{Co}} \cdot \text{s}$ in the absence of cobalt particle size effects. Consequently, the deactivation based on loss of surface area amounts to 73%, even higher than the measured rate of 52%. To estimate the degree of sintering in the spent catalyst a detailed TEM study was executed. In Figure 3 two HAADF images are presented clearly showing the large extent of sintering. The cobalt particles in the inner tube of the CNF material have sintered to a lesser extent up to 8 nm, which can be rationalized as the benefit of confinement against sintering.

From the cobalt particle size distribution presented in Figure 1b a surface mean particle size of 21 nm was calculated. The decrease

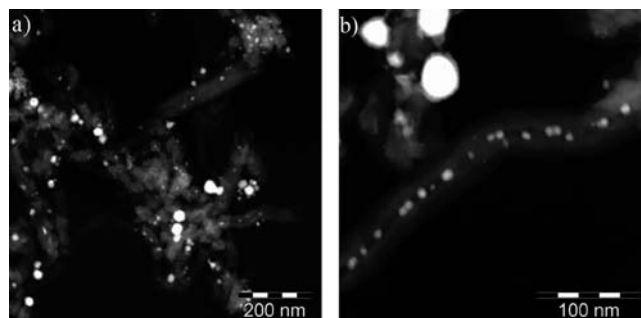


Figure 3. (a) Overview TEM image obtained with the HAADF detector of the spent catalyst. (b) More detailed image showing trapped more modestly sintered particles in the inner tube of the carbon nanofibers.

in metal dispersion was 77%, in quantitative agreement with measured deactivation. Regarding the mechanism of sintering, noteworthy is the presence of several areas in the TEM images where sintered particles are in close proximity, sometimes even making contact. Based on that observation we conclude that particle coalescence has taken place, but the data do not allow excluding Ostwald ripening. We rationalize the large impact of RH on sintering behavior by the presence of cobalt hydroxyl groups that enable free movement of particles over the wetted support. The direct evidence that detrimental effects of water on FT performance were not related to bulk oxidation of cobalt nanoparticles, but to water enhanced sintering, is very relevant for FT research. In our future work we plan to extend these findings to commonly applied oxidic support materials.

Acknowledgment. We are grateful to Dr. Johan den Breejen (Utrecht University) for supplying the CNF support and to professor John Geus for the measurement of the TEM images.

Supporting Information Available: Full details on catalyst preparation, characterization, and Mössbauer measurements. This material is available free of charge via the Internet at <http://pubs.acs.org>.

References

- (1) (a) Colley, S. E.; Copperthwaite, R. G.; Hutchings, G. J.; Terblanche, S. P.; Thackeray, M. M. *Nature* **1989**, *339*, 129–130. (b) Jenkins, S. J.; King, D. A. *J. Am. Chem. Soc.* **2000**, *122*, 10610–10614.
- (2) Moodley, D. J.; Van de Loosdrecht, J.; Saib, A. M.; Niemantsverdriet, J. W. In *Advances in Fischer–Tropsch Synthesis, Catalysts, and Catalysis*; Davis, B. H., Ocelli, M. L., Eds.; CRC Press: Boca Raton, FL, 2010; pp 49–81.
- (3) (a) Jacobs, G.; Patterson, P. M.; Das, T. K.; Luo, M.; Davis, B. H. *Appl. Catal., A* **2004**, *270*, 65–76. (b) Van de Loosdrecht, J.; Balzhinimaev, B.; Dalmon, J. -A.; Niemantsverdriet, J. W.; Tsybulya, S. V.; Saib, A. M.; van Berge, P. J.; Visagie, J. L. *Catal. Today* **2007**, *123*, 293–302.
- (4) (a) Bezemer, G. L.; Bitter, J. H.; Kuipers, H. P. C. E.; Oosterbeek, H.; Holewijn, J. E.; Xu, X.; Kapteijn, F.; Van Dillen, A. J.; De Jong, K. P. *J. Am. Chem. Soc.* **2006**, *128*, 3956–3964. (b) Den Breejen, J. P.; Radstake, P. B.; Bezemer, G. L.; Bitter, J. H.; Frøseth, V.; Holmen, A.; De Jong, K. P. *J. Am. Chem. Soc.* **2009**, *131*, 7197–7203.
- (5) Winter, F.; Bezemer, G. L.; Van der Spek, C.; Meeldijk, J. D.; Van Dillen, A. J.; Geus, J. W.; De Jong, K. P. *Carbon* **2005**, *43*, 327–332.
- (6) Bødker, F.; Mørup, S.; Pedersen, M. S.; Svedlindh, P.; Jonsson, G. T.; Garcia-Palacios, J. L.; Lazaro, F. J. *J. Magn. Magn. Mater.* **1998**, *925*, 177–181.

JA103002K